

Review

# Overview of Silica-Polymer Nanostructures for Waterborne High-Performance Coatings

Tiago D. Martins, Tânia Ribeiro  and José Paulo S. Farinha \* 

Centro de Química Estrutural, Department of Chemical Engineering, Instituto Superior Técnico, Universidade de Lisboa, 1049-001 Lisboa, Portugal; tiagodmartins@tecnico.ulisboa.pt (T.D.M.); tania.ribeiro@tecnico.ulisboa.pt (T.R.)

\* Correspondence: farinha@tecnico.ulisboa.pt

**Abstract:** Combining organic and inorganic components at a nanoscale is an effective way to obtain high performance coating materials with excellent chemical and physical properties. This review focuses on recent approaches to prepare hybrid nanostructured waterborne coating materials combining the mechanical properties and versatility of silica as the inorganic filler, with the flexural properties and ease of processing of the polymer matrix. We cover silica-polymer coupling agents used to link the organic and inorganic components, the formation of hybrid films from these silica-polymer nanostructures, and their different applications. These hybrid nanostructures can be used to prepare high performance functional coatings with different properties from optical transparency, to resistance to temperature, hydrophobicity, anti-corrosion, resistance to scratch, and antimicrobial activity.

**Keywords:** silica-polymer nanostructures; high performance hybrid films; functional waterborne coatings



**Citation:** Martins, T.D.; Ribeiro, T.; Farinha, J.P.S. Overview of Silica-Polymer Nanostructures for Waterborne High-Performance Coatings. *Polymers* **2021**, *13*, 1003. <https://doi.org/10.3390/polym13071003>

Academic Editor: Andreea Groza

Received: 1 March 2021

Accepted: 22 March 2021

Published: 24 March 2021

**Publisher's Note:** MDPI stays neutral with regard to jurisdictional claims in published maps and institutional affiliations.



**Copyright:** © 2021 by the authors. Licensee MDPI, Basel, Switzerland. This article is an open access article distributed under the terms and conditions of the Creative Commons Attribution (CC BY) license (<https://creativecommons.org/licenses/by/4.0/>).

## 1. Introduction

The field of polymer coatings has a huge societal impact [1]. Polymer coatings are used all around us, for the decoration and protection of surfaces, but more importantly to give them different functionalities. Waterborne polymer coatings assume special importance because of their lower environmental impact, due to the use of much lower amounts of volatile organic compounds (VOCs). VOCs are used to facilitate polymer interdiffusion during film formation so as to produce a stronger film upon evaporation. Although the coatings industry have been reducing the use of VOCs [2–4], waterborne coatings based on dispersions of polymer nanoparticles (PNPs), also known as latex, do not easily reach the high performance of their solventborne counterparts [5].

### 1.1. Film Formation in Waterborne Coatings

Waterborne polymer coatings are formed in three steps: Evaporation of the solvent (water), deformation of the PNPs, and coalescence by interdiffusion of the polymer chains (Figure 1). Water evaporation leads to a close-packed layer of PNPs and the deformation of the particles from their spherical shape (by a combination of capillary, osmotic, and surface forces), above the “minimum film formation temperature” ( $T_{mff}$ , which is close to the glass transition temperature,  $T_g$ , of the polymer in water) [5–8], to produce a continuous but still mechanically weak film. Coalescence of the nanoparticles by polymer chain interdiffusion across the particle boundaries (above the polymer  $T_g$ ) produce the final mechanically resistant film [9–11]. The mechanical performance of the material depends on the degree of entanglement between polymer chains from across particle boundaries.

Diffusion of polymer chains across nanoparticle boundaries is of paramount importance in the formation of a film with good mechanical properties. The most common techniques to follow diffusion of the polymer chains across the interface between polymer nanoparticles (PNPs) in waterborne films are small angle neutron scattering (SANS) and Förster resonance energy transfer (FRET). SANS experiments can be used to measure the

relation between the extent of diffusion and the film tensile strength [12,13], however they require the cumbersome preparation of deuterated and nondeuterated PNPs to obtain the necessary contrast. Measurement of polymer interdiffusion by FRET, on the other hand, requires the labeling of PNPs with appropriate dyes: A fluorescent energy donor and an energy acceptor [14]. FRET can give information on the mixing of polymers labeled with donor and acceptor dyes in a wide range geometries [15–18], allowing the experimental determination of dye concentration profiles in complex nanostructured materials [19]. FRET has been used to study the effects of different factors on the formation of waterborne coatings, such as curing temperature [20], plasticizers [21], blending [22], crosslinkers [23–25], and the presence of filler particles [26–29].

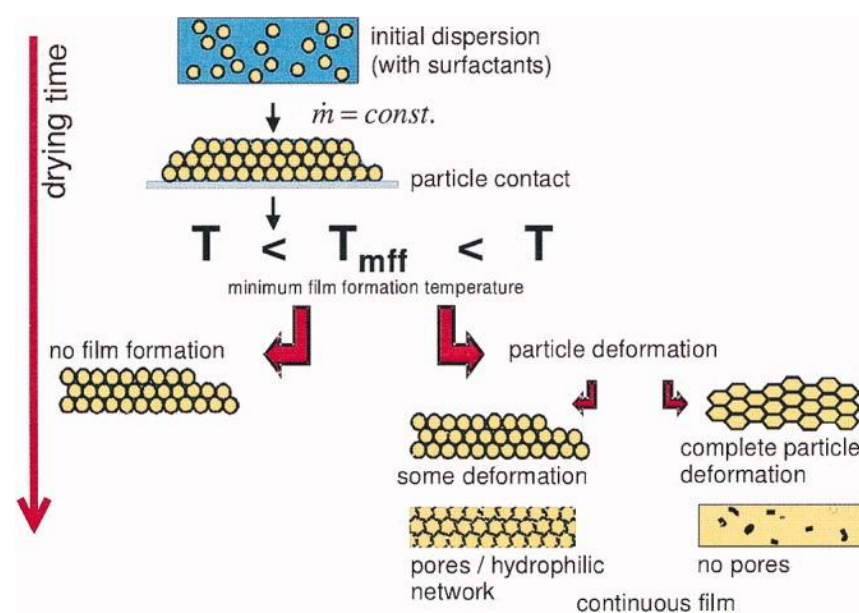


**Figure 1.** Film formation from water dispersions of polymer nanoparticles (PNPs). Water evaporation leads to a PNP packing, which deform above a minimum film formation temperature ( $T_{mff}$ ), as a result of surface tension and capillary forces. Complete particle deformation and chain interdiffusion at  $T > T_g$  leads to a continuous non-porous film. Reprinted with permission from ref. [8]. Copyright 2007 American Institute of Chemical Engineers (AIChE).

For these experiments, the films are prepared from a blend of FRET donor- and acceptor-labeled PNPs, for which the fluorescence spectra of the donor overlaps the absorption spectra of the acceptor. Since the molar fraction of the dyes is very low, it is assumed that the donor and acceptor dyes serve only as tracers for the location of the polymer. Since donor and acceptor dyes are located in different particles, FRET measurements can be used to evaluate the extent of mixing during the formation of the polymer film [30,31].

In the process of film formation from waterborne polymer coatings, there is an inherent trade-off between the kinetics of diffusion and the mechanical resistance of the final film. Using polymers with lower molecular weight and/or lower  $T_g$  leads to faster polymer interdiffusion, but a final film with lower mechanical resistance. However, using polymers with higher molecular weight and/or higher  $T_g$  does not necessarily produce better films because interdiffusion of the polymer chains can be strongly hindered, ultimately producing brittle films.

The traditional approach to this conundrum was to add VOCs as plasticizers to promote faster diffusion by decreasing the  $T_g$  of polymer only during film formation. Since the VOCs evaporate from the final film, this allows the use of polymers with a larger molecular weight and higher  $T_g$  that result in films with better mechanical resistance. The complete elimination of VOCs from waterborne polymer coating compositions requires new strategies to improve film mechanical resistance. The most promising approaches

rely in balancing polymer diffusion with chain crosslinking and incorporating inorganic components in the film, notably silica nanoparticles (SNPs).

### 1.2. Diffusion and Crosslinking

Crosslinking of the diffusing polymer chains during film formation can be used to anchor the chains and thus increase mechanical resistance. Covalent bonding between chains diffusing out of the PNPs in the film form a polymer network that can increase the temperature, solvent, and mechanical resistance of the final films. This three-dimensional network not only reinforces the polymer matrix but also strengthens the interface with other components of the film. However, network formation is only effective if the polymer chains are able to diffuse before the crosslinking reaction takes place, so that film formation depends on the kinetics of both processes [23]. The balance between the diffusion and crosslinking kinetics has been theoretically modeled by De Gennes [6] to explain the role of diffusion and crosslinking on the development of the films and their final properties. The ratio of the diffusion time ( $T_{diff}$ , time for a chain to diffuse out of its initial conformation) and the reaction time ( $T_{reac}$ , time for one cross-link to form in each chain),  $\alpha = T_{diff}/T_{reac}$ , increases when the mobility of the chains is reduced upon crosslinking ( $\alpha \gg 1$ ), inhibiting the healing of the interfaces, which results in poor mechanical properties. If crosslinking happens after the significant diffusion of the polymer ( $\alpha \ll 1$ ), the resulting material will not present mechanical properties better than the bulk material. Careful balancing of crosslinking and interdiffusion ( $\alpha \approx 1$ ) is necessary to optimize the film's mechanical properties [5,6,32].

Crosslinking strategies usually consist in incorporating different reactive groups in different polymer nanoparticles, so that the reaction occurs only upon chain diffusion during film formation, thus preserving the dispersion stability. Different approaches have been used to implement this strategy. For example, dispersions containing *N*-methylacrylamide or *N*-ethylacrylamide have been studied (Figure 2A), but were found to produce byproducts that are either toxic (formaldehyde) or result in the formation of low molecular weight polymers with weak mechanical properties [7,33–35]. On the other hand, the use of the reversible keto-hydrazide crosslinking reaction (Figure 2B) resulted in a small improvement of the mechanical properties of the film because of its low reaction rate, and in addition, hydrazide has toxic effects [36–38]. Crosslinking between isocyanate-containing polymers (Figure 2C) resulted in insufficient interfacial crosslinking and thus, lack of mechanical strength [3]. The use of the Michael addition with diamines (Figure 2D) [39] was found to hinder chain diffusion, also yielding polymer films with poor mechanical properties.

### 1.3. Inorganic Nanofillers

A more promising approach to improve the performance of waterborne coatings without compromising the flexural properties of the polymer is the incorporation of nanosized inorganic components (or nanofillers). Although different fillers have been used in coating applications (Table 1) [40,41], silica nanoparticles (SNPs) have received special attention due to their high surface area, cost-effective production, and easy surface functionalization [42]. SNPs can be prepared by simple, scalable, and low-cost techniques and offer tunable and very well-defined size, morphology, and porosity. Hybrid-silica materials combine the rigidity and high thermal stability of the inorganic components with the flexibility, ductility, and processability of the polymer matrix [9]. When used in polymer coating formulations, SNPs can also add new functionalities to the films, providing protection from moisture, temperature, scratching, radiation, and corrosion, while preserving optical transparency and providing specific electrical or mechanical behavior, regulation of microbial adhesion, etc.

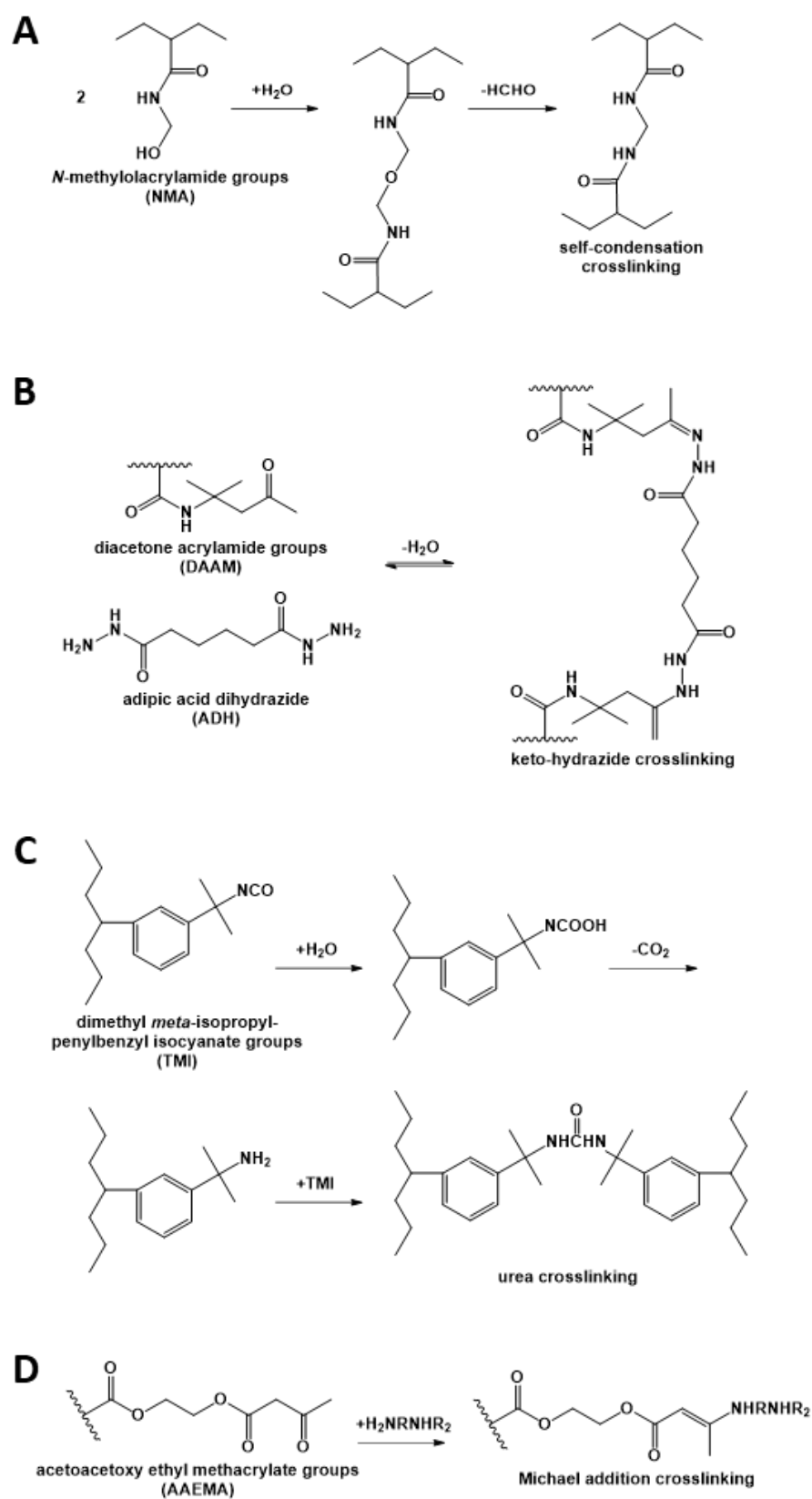


**Figure 2.** Crosslinking reactions used in waterborne polymer coatings, based on (A) *N*-methylolacrylamide; (B) diacetone acrylamide (DAAM) and adipic acid dihydrazide; (C) dimethyl *meta*-isopropenylbenzyl isocyanate (TMI); and (D) acetoacetoxy ethyl methacrylate (AAEMA) with a diamine.

**Table 1.** Inorganic fillers other than silica nanoparticles (SNPs) used in hybrid materials for coating applications.

Inorganic Filler	Organic Matrix	Properties	References
Clay	Polyimide	Adhesive strength, abrasion resistance, impact strength, water absorption resistance	[43,44]
	Epoxy	Abrasion resistance, water vapor barrier, corrosion resistance	[45,46]
Carbon Nanotubes	Epoxy	Tensile strength, electric insulation	[47,48]
Graphene Oxide	Poly(vinyl butyral)	Corrosion resistance, superhydrophobicity	[49]
	Epoxy	Corrosion resistance, superhydrophobicity	[50–53]
Zeolite	Epoxy	Corrosion resistance	[54]
TiO <sub>2</sub>	Metal-quinoline derivatives; poly(methyl methacrylate)	Corrosion resistance, low friction	[55,56]

In this review, we discuss recent progress in the preparation of high-performance coatings using silica-polymer hybrid nanomaterials, presenting the different silica nanostructures and their functionalization for incorporation into waterborne polymer coating materials. We summarize some of the strategies reported for the incorporation of silica nanostructures in polymeric matrixes in coating applications, and present recent results on functional coating applications based in hybrid waterborne polymer dispersions.

## 2. Preparation and Functionalization of Silica Nanostructures for Coating Applications

Silica nanoparticles (SNP) used in hybrid silica-polymer coatings are usually prepared by flame hydrolysis (fumed silica) or by the Stöber method (colloidal silica). Although fumed silica have a lower cost when compared to colloidal silica, it has a tendency to irreversibly aggregate [9]. Colloidal silica is obtained by the Stöber method, a sol-gel process based on the hydrolysis and condensation of silica precursors, such as tetraethyl orthosilicate (TEOS), in an aqueous medium at a basic pH [57]. High porosity mesoporous silica nanoparticles (MSNs) can be obtained by adding a template to the sol-gel (for example, cetyltrimethylammonium chloride—CTAC, cetyltrimethylammonium bromide—CTAB, or Pluronic F127). MSNs feature tunable diameter and pore size [58,59], and huge surface area and pore volume values that allow extensive and selective surface functionalization, as well as the loading of different cargo [60–63].

The use of MSNs in hybrid polymer coatings is mostly unexplored, but holds great promise [64–68]. For example, Shi et al. [67] prepared epoxy coatings loaded with MSNs as reservoirs for the corrosion inhibitor 8-hydroxyquinoline. Another study on wear resistance of epoxy coatings, showed that incorporation of MSNs loaded with 2-mercaptobenzothiazole (MBT) in the epoxy coatings improved the micro-hardness and decreased the friction coefficient of the coating, increasing its wear resistance [64]. Liu et al. [66] further showed the preparation of a mesoporous silica coating on graphene oxide nanosheets and its incorporation in styrene-butadiene rubber composites to improve their thermal conductivity.

### 2.1. Compatibilization of Silica Nanostructures with the Polymer Matrix

The incorporation of ca. 10 wt% of silica nanoparticles in polymer coating materials has been described to have the best impact in film properties [9,69–72]. However, this amount is sufficiently large to often produce significant aggregation of the polar silica nanostructures in the usually hydrophobic polymer matrix, leading to the aggregation of the particles, phase separation, and the formation of a mechanically weak composite.

Since homogeneous films with relatively high solids content are required for high performance waterborne coatings, SNP aggregation must be reduced in order to increase the silica content in the mixture. One strategy to achieve this is by functionalizing the silica surface (Figure 3) to increase the silica-polymer affinity (by promoting van der Waals forces, hydrogen bonds, or ionic interactions), or to covalently link the two components, maximizing the interfacial stability between the silica and polymeric matrix. This can be achieved by functionalizing the silica nanoparticles with a coupling agent that provides grafting of polymer chains onto the SNPs surface. Coupling agents should form siloxane

bonds with the SNPs via the hydrolysis and condensation of alkoxy groups, and bear functional groups to connect to the polymer matrix [9,69,70,73].

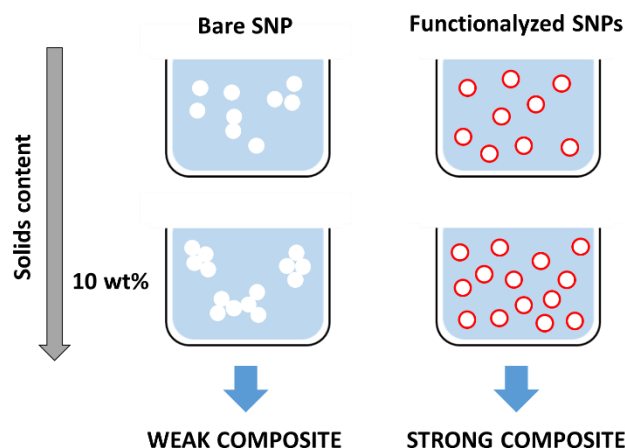


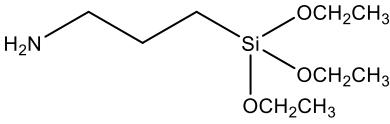
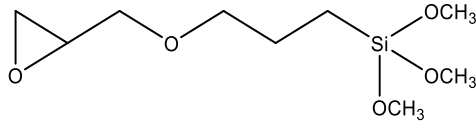
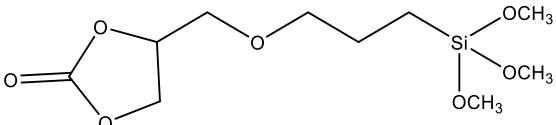
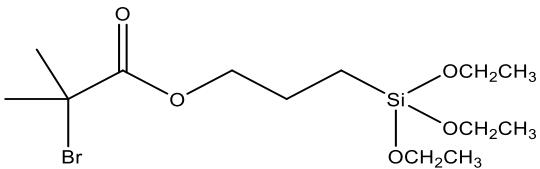
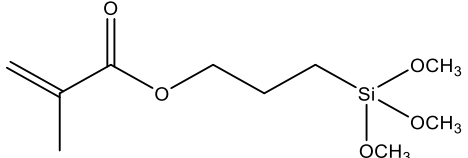
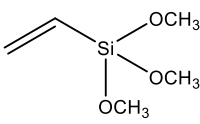
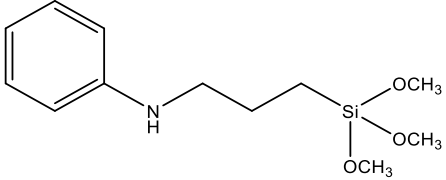
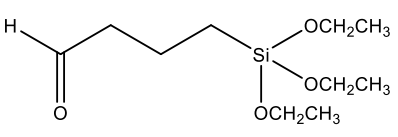
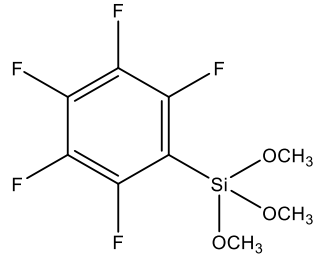
**Figure 3.** Optimization of hybrid coatings often involve the incorporation of up to ca. 10 wt% of SNPs in polymer material. At such solids content bare SNPs tend to aggregate, resulting in a weak composite (left). By appropriately functionalizing the SNPs (right), it is possible to obtain homogeneous distributions of the SNPs in the dispersion and polymer matrix, leading to better composite performance.

## 2.2. Silica-Polymer Coupling Agents

Coupling agents not only enhance the compatibility between the organic and inorganic components to obtain homogeneous dispersions and films, but can also avoid cavitation in the films due to the low interaction between the matrix and filler. Coupling agents should thus be chosen according to the polymeric matrix and the material's desired application. The main criteria for this choice are the ability to bind to the polymer of the matrix (for example, through a polymerizable group), while attaching to the silica network by alkoxy silane groups. Table 2 describes the most common coupling agents used in the preparation of silica-polymer nanostructures. For example, 3-aminopropyl triethoxysilane (APTES) is widely used to bind to epoxy resins [74–76] and polyurethane [77], increasing their performance, or even as grafting sites for RAFT agents [78] and ATRP initiators [79]. On the other hand, functionalizing SNPs with  $\gamma$ -(2,3-epoxypropoxy)propyl-trimethoxysilane (GPTMS) can increase the compatibility of the inorganic component within epoxy resins [80–84]. GPTMS can be further modified into carbonate functionalized silanes (4-((3-(trimethoxysilyl)propoxy)methyl)-1,3-dioxolan-2-one, CPS) increasing polyurethane-based coatings performance [85]. ATRP initiators are commercially available as silica precursors, for example 3-(2-Bromoisobutyryl)propyl triethoxysilane (BPTS) [86,87], for directly growing polymer chains in the silica surface.

Another strategy widely used to grow polymer chains from the silica surface is the functionalization with 3-Methacryloxypropyl trimethoxysilane (MPS), which provides anchoring to acrylic monomers, such as butyl methacrylate (BMA) [88,89], butyl acrylate (BA) [72,79,90], methyl methacrylate (MMA) [72,89,90], dodecafluoroheptyl methacrylate (DFMA) [72], bisphenol A-glycidyl methacrylate (Bis-GMA) [91], hexanedioldiacrylate (HDDA) [92], methacrylic acid (MAA) [93], benzyl methacrylate (BnMA), 2-hydroxyethyl methacrylate (HEMA) [94], glycidyl methacrylate (GMA) [95], and vinyl-bearing monomers like styrene (St) [79,96,97]. Increasing the compatibility between silica and styrene has also been performed using vinyltrimethoxysilane (VTMS) [96] or *N*-(3-(trimethoxysilyl)propyl)-aniline (PATMS) [98]. Although not used on coating materials yet, triethoxysilylbutyraldehyde (TEBA) can open a new route for covalently bonded hybrid materials [99].

**Table 2.** Most common coupling agents used in the preparation of hybrid silica-polymer materials.

	Name	Chemical Structure	Ref.
APTES	3-Aminopropyl triethoxysilane		[74–78]
GPTMS	3-Glycidoxypropyl trimethoxysilane		[80–84,100]
CPS	4-((3-(trimethoxysilyl)propoxy)methyl)-1,3-dioxolan-2-one		[85]
BPTS	3-(2-Bromoisobutyryl)propyl triethoxysilane		[86,87]
MPS	3-Methacryloxypropyl trimethoxysilane		[29,72,79,88–97]
VTMS	Vinyltrimethoxysilane		[96]
PATMS	N-[3-(trimethoxysilyl)propyl]aniline		[98]
TEBA	Triethoxysilylbutyraldehyde		[99]
PFPS	Pentafluorophenyltriethoxysilane		[101]

The effect of the coupling agent on the surface of SNPs is critical for specific properties of the polymer-silica nanostructure, such as its hydrophilicity, hydrophobicity, or chemical binding ability [5,73]. Zhi et al. [84] have functionalized the surface of the SNPs with GPTMS for better compatibility with epoxy resin. They were able to achieve strong bonds between the silica and polymer matrix, obtaining a nanometer-scale surface roughness that resulted in a superhydrophobic material. Jouyandeh et al. [100] worked on the functionalization of nanoparticles with nitrogen-rich macromolecules that would drive crosslinking reactions with pyromellitic acid dianhydride. In this case GPTMS was used to firstly bind the super reactive hyperbranched polyethylenimine (PEI) that would later be grafted on the silica surface, significantly improving the performance of the material. Xu et al. [101] functionalized SNPs with pentafluorophenyltriethoxysilane (PFPS), enabling its dispersion within hyperbranched fluoropolymer (HBFP). The chemically modified silica nanoparticles presented reactive functionalities that were later covalently integrated into the complex networks.

A completely different approach to enhance the compatibility within the hybrid material was developed by Kumar et al., who modified the SNPs surface with  $^{60}\text{Co}$ -gamma radiation to induce the grafting of GMA and HEMA. This effectively increased the compatibility of the SNP with the vinyl polymeric matrix, increasing the performance of the coating [102].

### 3. Incorporation of Silica in Polymer Materials

The more common methods to prepare hybrid organic/inorganic coating materials are (Figure 4): (1) The combination of the polymer chains or polymer nanoparticles with the inorganic nanoparticles; (2) the polymerization of the organic component in the presence of inorganic nanoparticles; (3) the formation of the inorganic component in the presence of the polymer chains or nanoparticles; and (4) the simultaneous formation of both polymer and inorganic components [103].

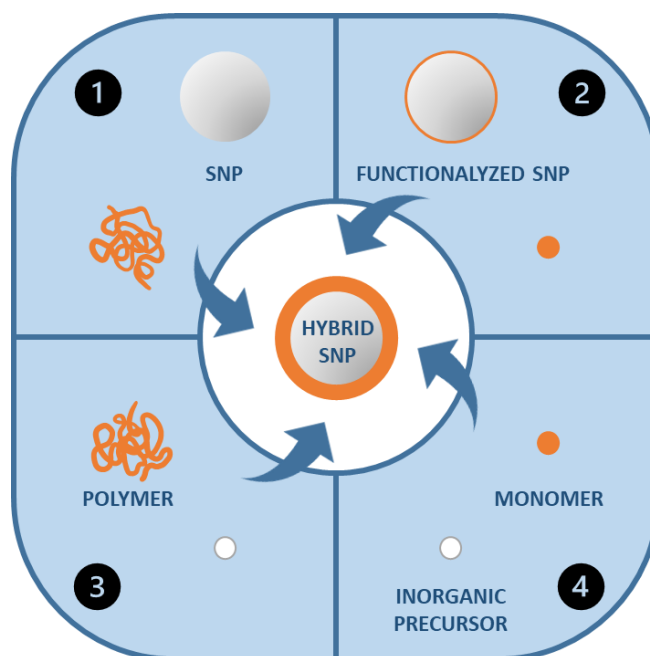


**Figure 4.** Different synthetic strategies for the formation of polymer-silica hybrid nanoparticles.

While (1) can lead to the aggregation of the inorganic component and phase separations as discussed above, and (3) and (4) do not offer general processing advantages, strategy (2) allows the preparation of very homogeneous hybrid polymer films. This approach can involve emulsion polymerization in the presence of inorganic nanoparticles [29,88] or the modification of surface functionalized inorganic particles with polymer chains (see above) to promote their homogeneous dispersion in the matrix. In the last



case, the polymer can be “grafted from” the surface of the inorganic nanoparticles [79,104] or “grafted to” the nanoparticles [79] (Figure 5) among other less used possibilities [105]. In the “grafting from” approach, the polymer chains grow from reactive groups on the surface of the inorganic nanoparticles. In the “grafting to” approach, the polymer chains are previously formed in solution and covalently bonded to the surface of the inorganic nanoparticles [103,106]. The “grafting from” method is generally believed to produce higher polymer density, but “grafting to” allows a more uniform coverage of the surface.

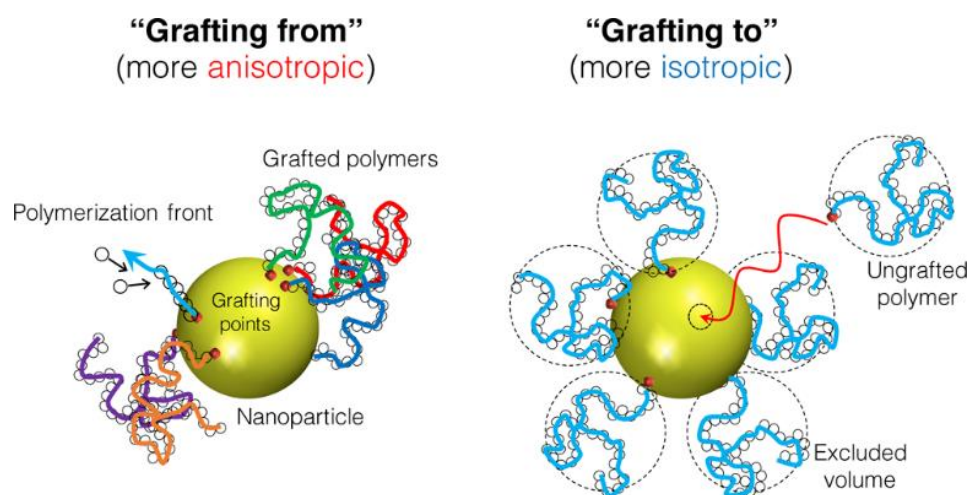


**Figure 5.** Surface coverage by “grafting from” and “grafting to” approaches. Reprinted with permission from ref. [106]. Copyright 2017 ACS.

In “grafting from” it is possible to use conventional free radical polymerization (on SNPs surface-modified with monomer units), or a controlled radical polymerization technique to control the composition, molecular weight, and molecular weight dispersity of the chains [107,108]. Atom transfer radical polymerization (ATRP) and reversible addition–fragmentation chain transfer (RAFT), are the most used techniques for a precise design of the polymer chains. While in ATRP, the SNP surface is modified with the initiator [79,109], in RAFT the surface of the SNPs is modified with a chain transfer agent (CTA) [61,97,110,111].

Another approach involves encapsulation of the SNP by emulsion polymerization. In this case, the SNPs are usually surface-modified with monomer units so that these can be used as seeding particles in the emulsion/mini-emulsion polymerization, effectively reducing SNP aggregation in the final coatings (Figure 6) [29,74,75].

The work of Désert et al. [112] reports the controlled morphology of the seeded emulsion polymerization of styrene on functionalized SNPs presenting a cluster morphology. The silica concentration and the feeding process have a strong impact on the particle morphology, yielding cluster-like [112], snowman-like [113], raspberry-like [95,114,115], or encapsulated core-shell hybrid nanoparticles [103–105] (Figure 7). Among the different morphologies, some have had no application in hybrid coatings (i.e., cluster-like and snowman-like nanoparticles). However, the morphology of the nanoparticles can impact the properties to the coating as described for the raspberry structures that lead to superhydrophobic properties [84]. Nanoparticles with a core-shell morphology, usually provide the more homogeneous dispersion in the polymer matrix [116].

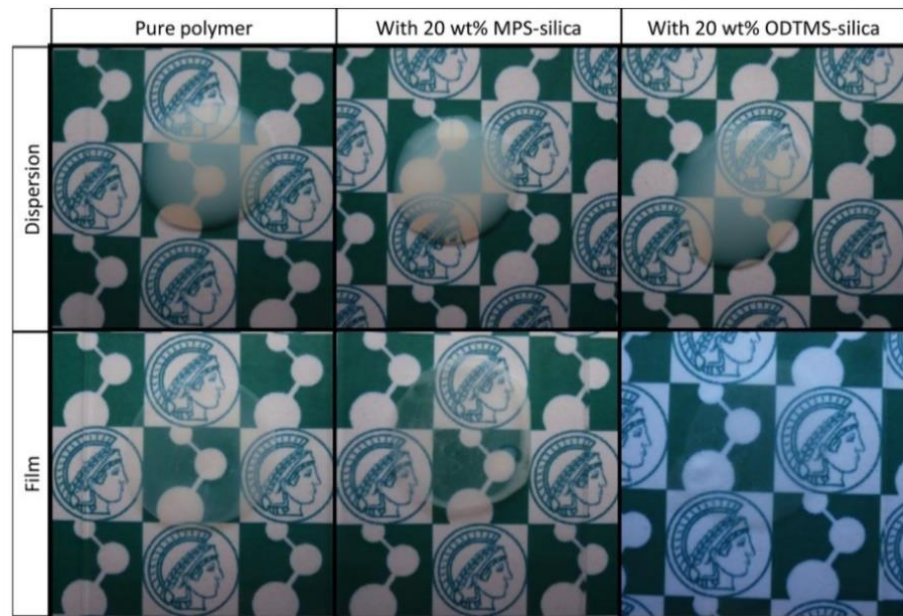


**Figure 6.** Dispersions (**top**) and the corresponding films annealing at 100 °C for 24 h (**bottom**) obtained using BMA:MMA (butyl methacrylate:methyl methacrylate) nanoparticles without silica (pure polymer), with 20 wt% of silica nanoparticles (SNPs) modified with MPS, and with 20 wt% of SNPs modified with ODTMS (N-octadecyltrimethoxysilane). Reprinted with permission from ref. [89]. Copyright 2016 John Wiley and Sons.

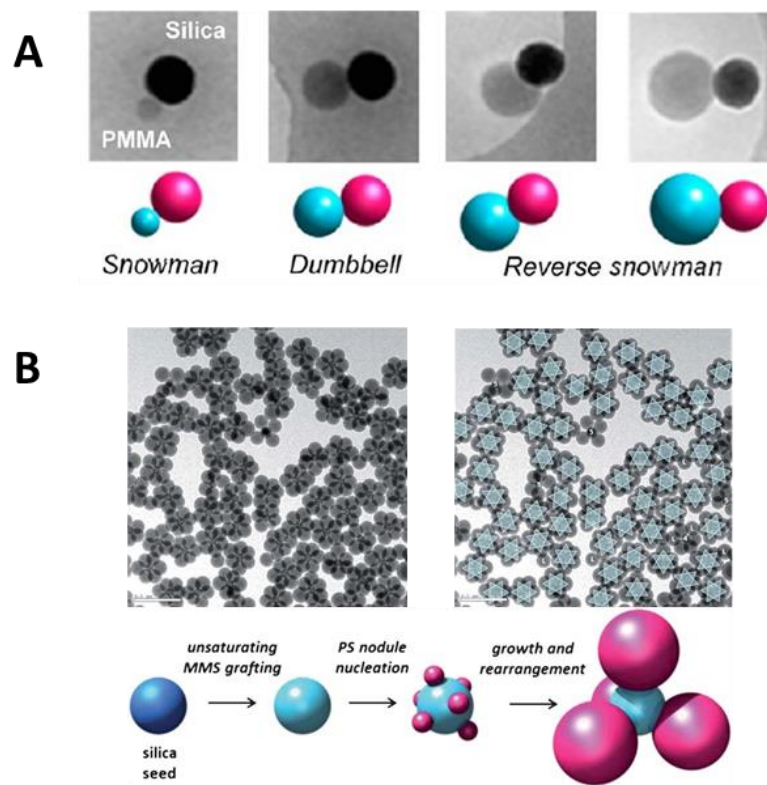


**Figure 7.** Cont.

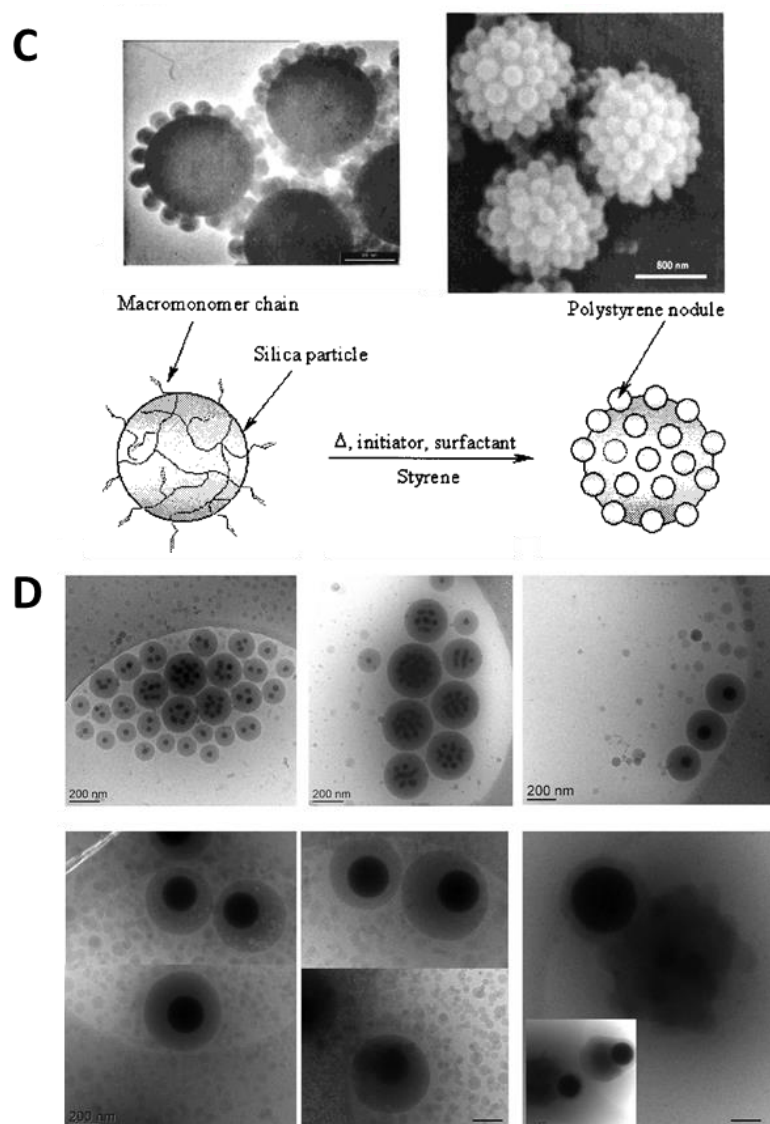


**Figure 7.** Hybrid particle morphology. (A) Dissymmetrical snowman- and dumbbell-like silica/polymer colloidal particles through emulsion polymerization of MMA or St using bicationic initiator previously anchored on the silica surface. Reprinted with permission from ref. [113]. Copyright 2012 ACS. (B) Hexapods obtained by St emulsion polymerization. Reprinted with permission from ref. [112]. Copyright 2012 The Royal Society of Chemistry. (C) Raspberry-like hybrids based on 1- $\mu\text{m}$  silica particles. Reprinted with permission from ref. [114]. Copyright 2002 ACS. (D) Encapsulated SNPs showing the effect of the SNPs size on the morphology of the hybrid particles (scale bar: 200 nm). Reprinted with permission from ref. [116]. Copyright 2016 ACS.

The surfactants used in emulsion polymerization can however have negative effects on the final properties and appearance of the coatings. Examples of surfactant-free emulsion polymerization for the encapsulation of SNPs include the combination of RAFT with emulsion polymerization, using a macro-RAFT agent that adsorbs onto the surface of the SNPs (Figure 8) [116] and the use of ionic comonomers (the sodium salt of styrene sulfonic acid and potassium methacrylate) to stabilize SNPs functionalized with MPS, to which poly(MMA-co-BA) was grafted [90].

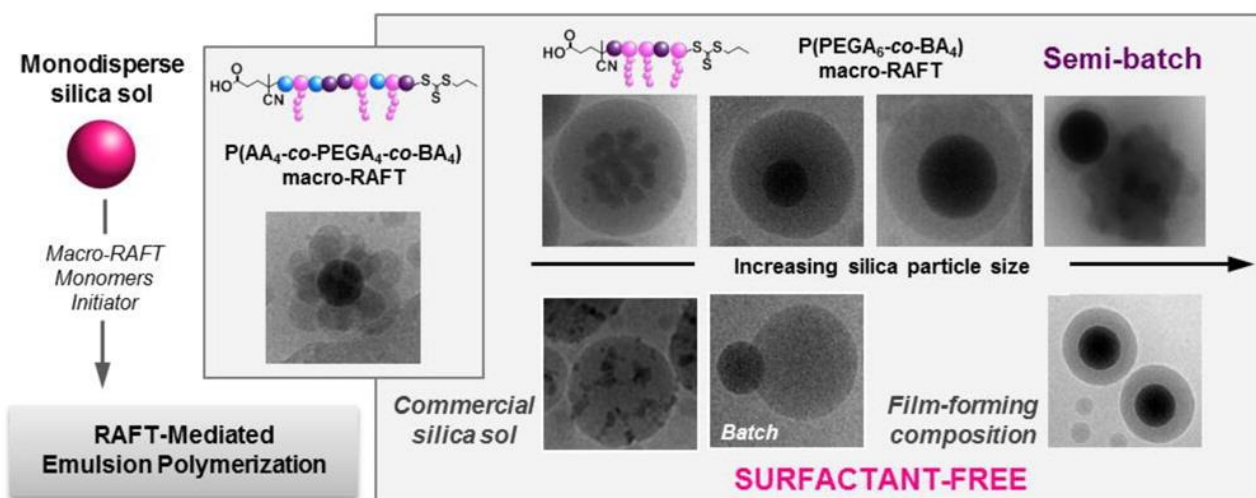


**Figure 8.** Illustration for the formation processes hybrid latexes by surfactant-free RAFT-mediated emulsion polymerization. Reprinted with permission from ref. [116]. Copyright 2016 ACS.

#### 4. Applications of Hybrid Nanostructured Films

Hybrid nanoparticles offer huge design flexibility for the design of coatings with a wide range of properties, improving not only the mechanical properties (e.g., impact, abrasion, or scratch) and chemical resistance (e.g., against oxidation and hydrolysis resulting from exposure to sunlight, air, and water), but also providing new functionalities (Table 3) [4,9]. Desirable properties in waterborne coatings include flexibility [29,88,117], adhesion [81,118,119], wear resistance [92,102,120–122], and durability [120]. Among the possibilities for added coating functionality are, for example, flame retardancy [119], solvent and chemical resistance [123,124], stain resistance [102,124], anti-cavitation [81], extreme robustness (for space-based applications) [125], antimicrobial activity [126–131], superhydrophobicity [84,95,124,132–138], or photoactive fluorescent coatings [29] presented in Table 3.

Often, the use of SNPs can improve different coating properties and simultaneously add new functionalities. For example, SNPs increase the  $T_g$  and hardness of polyurethane composite films, containing ethylene glycol methacrylate phosphate (EGMP), with the resulting material presenting also good adhesion to steel surfaces and flame retardancy [119]. In fact, silica-containing epoxy composites are already used in adhesives, paints, solvent and chemical resistance, and marine coating technology [118,123,130]. The use of 3-glycidyloxypropyl trimethoxysilane (GPTMS) and TEOS on epoxy composites lead to coating films with improved break resistance due to the hyperbranched structure of GPTMS, but also increased thermal stability and erosion resistance, for anti-cavitation coating applications [81]. SNPs modified with toluene diisocyanate (TDI) groups were used in high performance phenylene sulphide (PPS) nanocomposite coatings showing increased tensile strength and hardness [121].

Although the introduction of SNPs can increase the mechanical properties of coating materials, SNPs can also show negative effects on the final coatings. For example, they can impact crosslinking reactions in the films and their curing kinetics. For example, the addition of SNPs to water-based alkyd coatings changed their autoxidation curing kinetics, depending on the morphology of the nanoparticles and their aggregation level [139].

Different functionalities can be imparted to hybrid nanocomposite coatings by using SNPs. For example, even though SNP are non-toxic (they are usually considered biocompatible and are endogenous to most living organisms), they have been used to be used to impart antibacterial properties to coatings by taking advantage of their ease of processability and surface functionalization to carry antibacterial agents. Yamashita et al. [131] described a silicone rubber coating with antimicrobial activity against *S. aureus* and *E. coli* containing hybrid nanoparticles with a silica core and a poly(p-styrene tributyl-

tetradecylphosphonium sulfate) shell. Silicone rubber containing SNPs grafted with poly(vinylbenzyltributylphosphonium chloride) also show antibacterial activity against *S. aureus*, *E. coli*, and *P. aeruginosa* [129]. The antibacterial activity is strong even at very low nanoparticle concentrations (0.1 wt%) in different formulations (silicone rubber, polystyrene, and commercial paints). Hybrid nanoparticles obtained by co-condensation of *N*-(3-triethoxysilylpropyl)-5,5-dimethylhydantoin and TEOS, followed by chlorination, showed excellent antimicrobial activities against *E. coli* and *S. aureus*, with good storage stability for application in coating materials [127]. Antibacterial behavior against the same strains was also obtained for coating formulations containing polyols from Linseed and Castor oils as the organic fillers and TEOS as the inorganic constituent [128]. The chemical structure of this biodegradable family of materials can suffer chemical transformations yielding low molecular weight polymeric materials useful for eco-friendly coatings [140,141].

**Table 3.** Examples of hybrid silica-polymer coating applications.

Applications	Organic Matrix	References
Flame retardancy	Polyurethane, EGMP <sup>a</sup>	[119]
Solvent and chemical resistance	Epoxy	[123,124]
Stain resistance	Epoxy	[102]
	PIT <sup>b</sup>	[124]
Anti-cavitation	Epoxy	[81]
Robustness	Phenylene Sulfide	[121]
	Nylon-6	[125]
Antimicrobial	PQDMAEMA <sup>c</sup> , PTMOSPMA <sup>d</sup>	[126]
	TS-DMH <sup>e</sup>	[127]
	Polyols	[128]
	PVBBPC <sup>f</sup> , Silicone rubber	[129]
	Epoxy	[130]
	PSBDPS <sup>g</sup>	[131]
Superhydrophobic	Epoxy	[84]
	Epoxy-functionalized methacrylate	[95]
	PIT <sup>b</sup>	[124]
	TSI-PDMAEMA-PS <sup>h</sup>	[132]
	Fluoroloakylsiloxane polymer	[133]
	Urethane acrylate	[134,135]
	PFCP <sup>i</sup> -based chlorosilane	[136]
	DFMA <sup>j</sup>	[137]
Poly(methyl hydrosiloxane)	[138]	
Photoactive, fluorescent	Poly(butyl methacrylate)	[29]

<sup>a</sup> Ethylene glycol methacrylate phosphate; <sup>b</sup> poly(isobutylmethacrylate-co-3-methacryloxypropyltrimethoxysilane); <sup>c</sup> poly(2-(dimethylamino)ethyl methacrylate); <sup>d</sup> poly-(3-(trimethoxysilyl)propyl methacrylate); <sup>e</sup> *N*-(3-triethoxysilylpropyl)-5,5-dimethylhydantoin; <sup>f</sup> poly(vinylbenzyltributylphosphonium chloride); <sup>g</sup> poly(*p*-styrene tributyltetradecylphosphonium sulfate); <sup>h</sup> trimethoxysilane-end-capped poly(dimethylaminoethyl methacrylate)-block-polystyrene; <sup>i</sup> perfluorocyclopentene; <sup>j</sup> dodecafluoroheptyl methacrylate.

Nano-structuring of the coating film surface by the SNP has been explored to impart superhydrophobicity to coatings. This is an extremely interesting property, with application in self-cleaning, anticorrosion, antipollution, self-healing, and ice repellent surfaces [142]. Coatings with contact angles above 150° have been prepared using nanoparticles modified with different hydrophobic groups (e.g., fluorinated) [124,133–136,138] and modulating the roughness of the surface (e.g., using raspberry-like structures) [95,115,132]. Nahum et al. prepared nanocomposite coatings based on urethane acrylate and epoxy, containing SNPs functionalized with photoreactive benzophenone groups and a fluorinated silane [134]. These coatings are UV-cured to yield high contact angles and a

good bonding between the SNPs and polymeric matrix. Water-repellent fluorine-free coatings were also reported, based on nanostructured roughness provided by the incorporation of SNP in polyester [124]. After treatment with poly(isobutylmethacrylate-co-3-methacryloxypropyltri-methoxysilane) (PIT), hydrophobic polyester fabrics with good water repellence were obtained (Figure 9).

SNPs not only feature high chemical and mechanical stability, but also have the ability to protect guest molecules incorporated in the silica structure. They offer an excellent support for photoactive molecules since they are transparent in a wide range of wavelengths, from the ultraviolet to the near infrared (NIR), and they shield the dyes from oxygen, enhancing their photostability [29]. For example, fluorescent waterborne coatings were prepared from nanoparticles with a silica core and a polymer shell that originates from the coating film [88]. The SNPs were modified by the incorporation of a perylene diimide (PDI) derivative covalently linked to the silica network during the synthesis of the SNPs. The silica shields the dyes from oxygen, increasing their photostability, while the anchoring groups reduce dye aggregation and consequent fluorescence quenching. The SNPs surface was modified with MPS to graft a poly(butyl methacrylate) shell by emulsion polymerization. The hybrid particles yield films with good flexibility and transparency, strong fluorescence emission, and high mechanical strength (Figure 10). Compared to the films without the SNPs, those with hybrid nanoparticles have improved mechanical strength and higher  $T_g$  due to the lower polymer mobility [29,143].

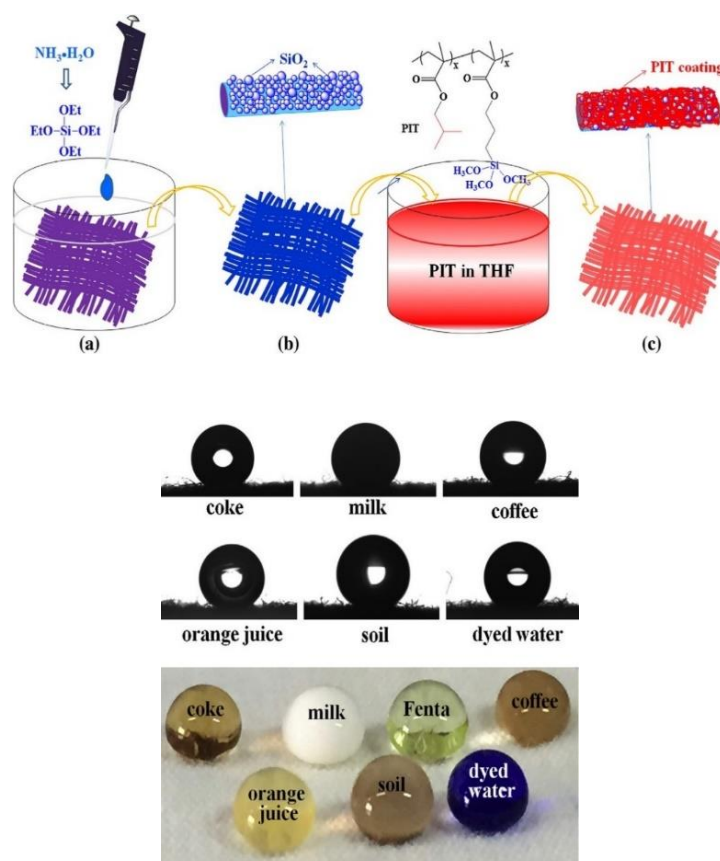


**Figure 9.** Hydrophobization of fabric with silica and polymeric water-repellent PIT. (a) Alkali-treated polyester fabric, (b)  $\text{SiO}_2$ @fabric, and (c) PIT hydrophobized  $\text{SiO}_2$ @fabric. The anti-stain properties of the fabric are observed upon trial with several aqueous mixtures (bottom). Reprinted with permission from ref. [124]. Copyright 2017 Elsevier.

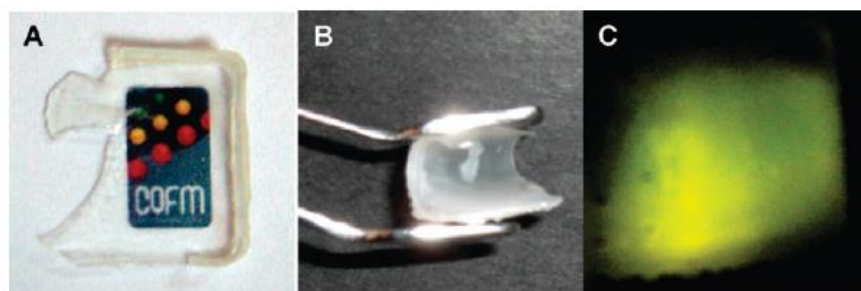


**Figure 10.** Hybrid film showing transparency (A), flexibility (B), and strong fluorescence emission under excitation at  $\lambda_{\text{exc}} = 450 \text{ nm}$  (C). Reprinted with permission from ref. [88]. Copyright 2009 ACS.

## 5. Conclusions and Outlook

The need to replace solvent-borne coatings by environmentally friendly waterborne coatings without losing performance has led to the development of different hybrid coating solutions. Those containing silica nanoparticles (SNP) offer the opportunity to design coatings with good mechanical performance and also other properties, such as superhydrophobicity, anti-corrosion, antimicrobial activity, optical activity, etc.

The combination of polymer and SNPs can improve the mechanical properties and the chemical resistance of hybrid coatings, but also offers the flexibility to develop high-performance environmentally friendly coatings with a wide range of functions. In these types of materials, the properties and performance are highly dependent on the silica content and the homogeneity of nanoparticles distribution in the coating film. Therefore, coupling agents play a major role in the nanofiller incorporation. These agents contain both reactive groups to attach to the polymer component and to anchor to the SNPs. This approach is particularly interesting in obtaining core-shell nanostructures, with a silica core and a polymer shell, offering excellent control over the distribution of the inorganic component in the polymer matrix of the coating, providing better mechanical performance and avoiding cavitation. The versatility of the preparation and surface modification of SNPs provide the design flexibility to use them as vehicles to impart different functionalities for specific coating applications, from flame retardancy to antimicrobial properties or photoactivity. Other functions, based on the structuring of the coating film provided by the nanoparticles have attracted strong interest, namely to produce anti-stain and superhydrophobic coatings. Better control of the nano-structuring in hybrid coatings offer other still underexplored possibilities, such as the development of structural color.

Silica-polymer hybrid nanostructures still hold untapped potential for the development of high performance environmentally friendly functional coatings for a plethora of novel applications.

**Author Contributions:** Conceptualization, J.P.S.F. and T.D.M.; methodology, J.P.S.F.; resources, J.P.S.F.; writing—original draft preparation, T.D.M.; writing—review and editing, J.P.S.F., T.R. and T.D.M.; supervision, J.P.S.F.; project administration, J.P.S.F.; funding acquisition, J.P.S.F. All authors have read and agreed to the published version of the manuscript.

**Funding:** This work was funded by Fundação para a Ciência e a Tecnologia (FCT-Portugal) and COMPETE (FEDER) within projects UIDB/00100/2020 and PTDC/CTM-POL/3698/2014. T.D.M. also thanks FCT for a PhD grant (SFRH/BD/132486/2017).

**Institutional Review Board Statement:** Not applicable.

**Informed Consent Statement:** Not applicable.

**Conflicts of Interest:** The authors declare no conflict of interest.

## References

1. Rezaei, S.D.; Shannigrahi, S.; Ramakrishna, S. A review of conventional, advanced, and smart glazing technologies and materials for improving indoor environment. *Sol. Energy Mater. Sol. Cells* **2017**, *159*, 26–51. [[CrossRef](#)]
2. Zeno, W.; Wicks, J.; Jones, F.N.; Pappas, S.P.; Wicks, D.A. *Organic Coatings Science and Technology*, 3rd ed.; Wiley-Interscience: Hoboken, NJ, USA, 1985; Volume 13, ISBN 9780471698067.
3. Yoon, J.; Lovell, P.A. Model reaction studies and crosslinking of dimethyl-meta-isopropenylbenzyl isocyanate containing ambient crosslinkable latex. *Macromol. Chem. Phys.* **2008**, *209*, 279–289. [[CrossRef](#)]
4. Jones, F.N.; Nichols, M.E.; Pappas, S.P. *Organic Coatings Science and Technology*, 4th ed.; Wiley: Hoboken, NJ, USA, 2017; ISBN 9780471698067.
5. Farinha, J.P.S.; Piçarra, S.; Baleizão, C.; Martinho, J.M.G. Smart Polymer Nanoparticles for High-Performance Water-Based Coatings. In *Industrial Applications for Intelligent Polymers and Coatings*; Springer: Cham, Switzerland, 2016; pp. 619–645. ISBN 978-3-319-26891-0.
6. Aradian, A.; Raphaël, E.; De Gennes, P.G. A scaling theory of the competition between interdiffusion and cross-linking at polymer interfaces. *Macromolecules* **2002**, *35*, 4036–4043. [[CrossRef](#)]
7. Taylor, J.W.; Winnik, M.A. Functional latex and thermoset latex films. *J. Coat. Technol. Res.* **2004**, *1*, 163–190. [[CrossRef](#)]
8. Ludwig, I.; Schabel, W.; Kind, M.; Castaing, J.-C.; Ferlin, P. Drying and Film Formation of Industrial Waterborne Latexes. *AIChE J.* **2006**, *53*, 549–560. [[CrossRef](#)]
9. Ribeiro, T.; Baleizão, C.; Farinha, J.P.S. Functional films from silica/polymer nanoparticles. *Materials* **2014**, *7*, 3881–3900. [[CrossRef](#)] [[PubMed](#)]
10. Chevalier, Y.; Pichot, C.; Graillat, C.; Joanicot, M.; Wong, K.; Maquet, J.; Lindner, P.; Cabane, B. Film formation with latex particles. *Colloid Polym. Sci.* **1992**, *270*, 806–821. [[CrossRef](#)]
11. Steward, P.A.; Hearn, J.; Wilkinson, M.C. Overview of polymer latex film formation and properties. *Adv. Colloid Interface Sci.* **2000**, *86*, 195–267. [[CrossRef](#)]
12. Hahn, K.; Ley, G.; Oberthür, R. On particle coalescence in latex films (II). *Colloid Polym. Sci.* **1988**, *266*, 631–639. [[CrossRef](#)]
13. Yoo, J.N.; Sperling, S.L.H.; Glinka, C.J.; Kleina, A. Characterization of Film Formation from Polystyrene Latex Particles via SANS. 2. High Molecular Weight. *Macromolecules* **1991**, *24*, 2868–2876. [[CrossRef](#)]
14. Winnik, M.A.; Wang, Y.; Haley, F. Latex film formation at the molecular level: The effect of coalescing aids on polymer diffusion. *J. Coat. Technol.* **1992**, *64*, 51–61.
15. Farinha, J.P.S.; Martinho, J.M.G.; Yekta, A.; Winnik, M.A. Direct Nonradiative Energy Transfer in Polymer Interphases: Fluorescence Decay Functions from Concentration Profiles Generated by Fickian Diffusion. *Macromolecules* **1995**, *28*, 6084–6088. [[CrossRef](#)]
16. Farinha, J.P.S.; Martinho, J.M.G. Electronic energy transfer in restricted geometries Application to the study of spherical and planar interphases of diblock copolymer films. *J. Lumin.* **1997**, *72–74*, 914–917. [[CrossRef](#)]
17. Yekta, A.; Winnik, M.A.; Farinha, J.P.S.; Martinho, J.M.G. Dipole-dipole electronic energy transfer. Fluorescence decay functions for arbitrary distributions of donors and acceptors. II. Systems with spherical symmetry. *J. Phys. Chem. A* **1997**, *101*, 1787–1792. [[CrossRef](#)]
18. Farinha, J.P.S.; Spiro, J.G.; Winnik, M.A. Dipole-dipole electronic energy transfer: Fluorescence decay functions for arbitrary distributions of donors and acceptors in systems with cylindrical symmetry. *J. Phys. Chem. B* **2004**, *108*, 16392–16400. [[CrossRef](#)]
19. Farinha, J.P.S.; Martinho, J.M.G. Resonance Energy Transfer in Polymer Interfaces. *Fluoresc. Supermol. Polym. Nanosyst.* **2008**, *4*, 215–255. [[CrossRef](#)]
20. Ye, X.; Farinha, J.P.S.; Oh, J.K.; Winnik, M.A.; Wu, C. Polymer diffusion in PBMA latex films using a polymerizable benzophenone derivative as an energy transfer acceptor. *Macromolecules* **2003**, *36*, 8749–8760. [[CrossRef](#)]
21. Farinha, J.P.S.; Martinho, J.M.G.; Kawaguchi, S.; Yekta, A.; Winnik, M.A. Latex film formation probed by nonradiative energy transfer: Effect of grafted and free poly(ethylene oxide) on a poly(n-butyl methacrylate) latex. *J. Phys. Chem.* **1996**, *100*, 12552–12558. [[CrossRef](#)]
22. Farinha, J.P.S.; Vorobyova, O.; Winnik, M.A. An energy transfer study of the interface thickness in blends of poly(butyl methacrylate) and poly(2-ethylhexyl methacrylate). *Macromolecules* **2000**, *33*, 5863–5873. [[CrossRef](#)]
23. Pham, H.H.; Farinha, J.P.S.; Winnik, M.A. Cross-linking, miscibility, and interface structure in blends of poly(2-ethylhexyl methacrylate) copolymers. An energy transfer study. *Macromolecules* **2000**, *33*, 5850–5862. [[CrossRef](#)]
24. Farinha, J.P.S.; Wu, J.; Winnik, M.A.; Farwaha, R.; Rademacher, J. Polymer diffusion in gel-containing poly(vinyl acetate-co-dibutyl maleate) latex films. *Macromolecules* **2005**, *38*, 4393–4402. [[CrossRef](#)]
25. Piçarra, S.; Afonso, C.A.M.; Kurteva, V.B.; Fedorov, A.; Martinho, J.M.G.; Farinha, J.P.S. The influence of nanoparticle architecture on latex film formation and healing properties. *J. Colloid Interface Sci.* **2012**, *368*, 21–33. [[CrossRef](#)]
26. Mizutani, T.; Arai, K.; Miyamoto, M.; Kimura, Y. Application of silica-containing nano-composite emulsion to wall paint: A new environmentally safe paint of high performance. *Prog. Org. Coat.* **2006**, *55*, 276–283. [[CrossRef](#)]
27. Kobayashi, M.; Rharbi, Y.; Brauge, L.; Cao, L.; Winnik, M.A. Effect of silica as fillers on polymer interdiffusion in poly(butyl methacrylate) latex films. *Macromolecules* **2002**, *35*, 7387–7399. [[CrossRef](#)]
28. Watanabe, M.; Tamai, T. Acrylic Polymer/Silica Organic-Inorganic Hybrid Emulsions for Coating Materials: Role of the Silane Coupling Agent. *J. Polym. Sci. Part A Polym. Chem.* **2006**, *44*, 4736–4742. [[CrossRef](#)]



29. Ribeiro, T.; Fedorov, A.; Baleizão, C.; Farinha, J.P.S. Formation of hybrid films from perylenediimide-labeled core-shell silica-polymer nanoparticles. *J. Colloid Interface Sci.* **2013**, *401*, 14–22. [[CrossRef](#)] [[PubMed](#)]
30. Martinho, J.M.G.; Farinha, J.P.S. Fluorescence Decay Methods for the Characterization of Latex Film Formation. *JCT Coat. Tech.* **2013**, *10*, 42–49.
31. Farinha, J.P.S.; Martinho, J.M.G. Resonance energy transfer in polymer nanodomains. *J. Phys. Chem. C* **2008**, *112*, 10591–10601. [[CrossRef](#)]
32. Ruch, F.; David, M.O.; Vallat, M.F. Adhesion in EPDM joints: Role of the interdiffusion mechanism on interfacial co-crosslinking. *J. Polym. Sci. Part B Polym. Phys.* **2000**, *38*, 3189–3199. [[CrossRef](#)]
33. Huang, S.R.; Lin, K.F.; Don, T.M.; Lee, C.F.; Wang, M.S.; Chiu, W.Y. Thermoresponsive conductive polymer composite thin film and fiber mat: Crosslinked PEDOT:PSS and P(NIPAAm-co-NMA) composite. *J. Polym. Sci. Part A Polym. Chem.* **2016**, *54*, 1078–1087. [[CrossRef](#)]
34. Garrett, R.Y. *Formaldehyde-Free, Self-Curing Interpolymers and Articles Prepared Therefrom*; U.S. Patent 5,021,529, 4 June 1991. U.S. Patent and Trademark Office: Washington, DC, USA, 1991.
35. Biale, G. *Self-Crosslinking Vinyl Acetate-Ethylene Latexes*; U.S. Patent 3,714,099, 30 January 1973. U.S. Patent and Trademark Office: Washington, DC, USA, 1973.
36. Machotova, J.; Podzimek, S.; Kvasnicka, P.; Zgoni, H.; Snuparek, J.; Cerny, M. Effect of molar mass on film-forming properties of self-crosslinking latexes based on structured acrylic microgels. *Prog. Org. Coat.* **2016**, *92*, 23–28. [[CrossRef](#)]
37. Hu, J.; Peng, K.; Guo, J.; Shan, D.; Kim, G.B.; Li, Q.; Gerhard, E.; Zhu, L.; Tu, W.; Lv, W.; et al. Click Cross-Linking-Improved Waterborne Polymers for Environment-Friendly Coatings and Adhesives. *ACS Appl. Mater. Interfaces* **2016**, *8*, 17499–17510. [[CrossRef](#)] [[PubMed](#)]
38. Zhang, X.; Liu, Y.; Huang, H.; Li, Y.; Chen, H. The Diacetone Acrylamide Crosslinking Reaction and Its Control of Core-Shell Polyacrylate Latices at Ambient Temperature. *J. Appl. Polym. Sci.* **2012**, *123*, 1822–1832. [[CrossRef](#)]
39. González, I.; Asua, J.M.; Leiza, J.R. Crosslinking in acetoacetoxy functional waterborne crosslinkable latexes. *Macromol. Symp.* **2006**, *243*, 53–62. [[CrossRef](#)]
40. Zhou, Y.; Liu, F.; Wang, H. Novel Organic-Inorganic Composites with High Thermal Conductivity for Electronic Packaging Applications: A Key Issue Review. *Polym. Compos.* **2017**, *38*, 803–813. [[CrossRef](#)]
41. Saveleva, M.S.; Eftekhari, K.; Abalymov, A.; Douglas, T.E.L.; Volodkin, D.; Parakhonskiy, B.V.; Skirtach, A.G. Hierarchy of hybrid materials—the place of inorganics-in-organics in it, their composition and applications. *Front. Chem.* **2019**, *7*, 179. [[CrossRef](#)]
42. Lee, D.W.; Yoo, B.R. Advanced silica/polymer composites: Materials and applications. *J. Ind. Eng. Chem.* **2016**, *38*, 1–12. [[CrossRef](#)]
43. Jena, K.K.; Raju, K.V.S.N.; Narayan, R.; Rout, T.K. Sodium montmorillonite clay loaded novel organic-inorganic hybrid composites: Synthesis and characterization. *Prog. Org. Coat.* **2012**, *75*, 33–37. [[CrossRef](#)]
44. Qiu, X.; Wang, H.; Zhou, C.; Li, D.; Liu, Y.; Yan, C. Polyimide/kaolinite composite films: Synthesis and characterization of mechanical, thermal and waterproof properties. *J. Taiwan Inst. Chem. Eng.* **2014**, *45*, 2021–2028. [[CrossRef](#)]
45. Madhup, M.K.; Shah, N.K.; Parekh, N.R. Investigation and improvement of abrasion resistance, water vapor barrier and anticorrosion properties of mixed clay epoxy nanocomposite coating. *Prog. Org. Coat.* **2017**, *102*, 186–193. [[CrossRef](#)]
46. Madhup, M.K.; Shah, N.K.; Parekh, N.R. An Investigation of Abrasion Resistance Property of Clay-Epoxy Nanocomposite Coating. *Mater. Sci. Res. India* **2018**, *15*, 165–178. [[CrossRef](#)]
47. Bakhtiar, N.S.A.A.; Akil, H.M.; Zakaria, M.R.; Kudus, M.H.A.; Othman, M.B.H. New generation of hybrid filler for producing epoxy nanocomposites with improved mechanical properties. *Mater. Des.* **2016**, *91*, 46–52. [[CrossRef](#)]
48. Wu, Z.; Gao, S.; Chen, L.; Jiang, D.; Shao, Q.; Zhang, B.; Zhai, Z.; Wang, C.; Zhao, M.; Ma, Y.; et al. Electrically Insulated Epoxy Nanocomposites Reinforced with Synergistic Core-Shell SiO<sub>2</sub>@MWCNTs and Montmorillonite Bifillers. *Macromol. Chem. Phys.* **2017**, *218*, 1700357. [[CrossRef](#)]
49. Zhu, G.; Cui, X.; Zhang, Y.; Chen, S.; Dong, M.; Liu, H.; Shao, Q.; Ding, T.; Wu, S.; Guo, Z. Poly (vinyl butyral)/Graphene oxide/poly (methylhydrosiloxane) nanocomposite coating for improved aluminum alloy anticorrosion. *Polymer (Guildf)* **2019**, *172*, 415–422. [[CrossRef](#)]
50. Ye, Y.; Zhang, D.; Liu, T.; Liu, Z.; Liu, W.; Pu, J.; Chen, H.; Zhao, H.; Li, X. Improvement of anticorrosion ability of epoxy matrix in simulate marine environment by filled with superhydrophobic POSS-GO nanosheets. *J. Hazard. Mater.* **2019**, *364*, 244–255. [[CrossRef](#)] [[PubMed](#)]
51. Ye, Y.; Zhang, D.; Li, J.; Liu, T.; Pu, J.; Zhao, H.; Wang, L. One-step synthesis of superhydrophobic polyhedral oligomeric silsesquioxane-graphene oxide and its application in anti-corrosion and anti-wear fields. *Corros. Sci.* **2019**, *147*, 9–21. [[CrossRef](#)]
52. Mohammadkhani, R.; Ramezanzadeh, M.; Saadatmandi, S.; Ramezanzadeh, B. Designing a dual-functional epoxy composite system with self-healing/barrier anti-corrosion performance using graphene oxide nano-scale platforms decorated with zinc doped-conductive polypyrrole nanoparticles with great environmental stability and non-tox. *Chem. Eng. J.* **2020**, *382*, 122819. [[CrossRef](#)]
53. Liu, C.; Qiu, S.; Du, P.; Zhao, H.; Wang, L. An ionic liquid-graphene oxide hybrid nanomaterial: Synthesis and anticorrosive applications. *Nanoscale* **2018**, *10*, 8115–8124. [[CrossRef](#)]
54. Rassouli, L.; Naderi, R.; Mahdavian, M. The role of micro/nano zeolites doped with zinc cations in the active protection of epoxy ester coating. *Appl. Surf. Sci.* **2017**, *423*, 571–583. [[CrossRef](#)]

55. Al Zoubi, W.; Ko, Y.G. Freestanding anticorrosion hybrid materials based on coordination interaction between metal-quinoline compounds and TiO<sub>2</sub>-MgO film. *J. Colloid Interface Sci.* **2020**, *565*, 86–95. [[CrossRef](#)]
56. Gu, G.; Zhang, Z.; Dang, H. Preparation and characterization of hydrophobic organic-inorganic composite thin films of PMMA/SiO<sub>2</sub>/TiO<sub>2</sub> with low friction coefficient. *Appl. Surf. Sci.* **2004**, *221*, 129–135. [[CrossRef](#)]
57. Stöber, W.; Fink, A.; Bohn, E. Controlled growth of monodisperse silica spheres in the micron size range. *J. Colloid Interface Sci.* **1968**, *26*, 62–69. [[CrossRef](#)]
58. Ribeiro, T.; Rodrigues, A.S.; Calderon, S.; Fidalgo, A.; Gonçalves, J.L.; André, V.; Duarte, M.T.; Ferreira, P.J.; Farinha, J.P.S.; Baleizão, C. Silica nanocarriers with user-defined precise diameters by controlled template self-assembly. *J. Colloid Interface Sci.* **2019**, *561*, 609–619. [[CrossRef](#)]
59. Calderon, V.S.; Ribeiro, T.; Farinha, J.P.S.; Baleizão, C.; Ferreira, P.J. On the Structure of Amorphous Mesoporous Silica Nanoparticles by Aberration-Corrected STEM. *Small* **2018**, *14*, 1802180. [[CrossRef](#)]
60. Croissant, J.G.; Fatieiev, Y.; Almalik, A.; Khashab, N.M. Mesoporous Silica and Organosilica Nanoparticles: Physical Chemistry, Biosafety, Delivery Strategies, and Biomedical Applications. *Adv. Healthc. Mater.* **2018**, *7*. [[CrossRef](#)] [[PubMed](#)]
61. Ribeiro, T.; Coutinho, E.; Rodrigues, A.S.; Baleizão, C.; Farinha, J.P.S. Hybrid mesoporous silica nanocarriers with thermoalve-regulated controlled release. *Nanoscale* **2017**, *9*, 13485–13494. [[CrossRef](#)] [[PubMed](#)]
62. Ahmad, H. Biocompatible SiO<sub>2</sub> in the Fabrication of Stimuli-Responsive Hybrid Composites and Their Application Potential. *J. Chem.* **2015**, *2015*, 846328. [[CrossRef](#)]
63. Moreno-Villaécija, M.Á.; Sedó-Vegara, J.; Guisasaola, E.; Baeza, A.; Regí, M.V.; Nador, F.; Ruiz-Molina, D. Polydopamine-like Coatings as Payload Gatekeepers for Mesoporous Silica Nanoparticles. *ACS Appl. Mater. Interfaces* **2018**, *10*, 7661–7669. [[CrossRef](#)]
64. Rahsepar, M.; Mohebbi, F. Enhancement of the wear resistance of epoxy coating in presence of MBT-loaded mesoporous silica nanocontainers. *Tribol. Int.* **2018**, *118*, 148–156. [[CrossRef](#)]
65. Mizoshita, N.; Tanaka, H. Versatile Antireflection Coating for Plastics: Partial Embedding of Mesoporous Silica Nanoparticles onto Substrate Surface. *ACS Appl. Mater. Interfaces* **2016**, *8*, 31330–31338. [[CrossRef](#)] [[PubMed](#)]
66. Liu, Z.; Zhang, H.; Song, S.; Zhang, Y. Improving thermal conductivity of styrene-butadiene rubber composites by incorporating mesoporous silica@solvothermal reduced graphene oxide hybrid nanosheets with low graphene content. *Compos. Sci. Technol.* **2017**, *150*, 174–180. [[CrossRef](#)]
67. Shi, H.; Wu, L.; Wang, J.; Liu, F.; Han, E.H. Sub-micrometer mesoporous silica containers for active protective coatings on AA 2024-T3. *Corros. Sci.* **2017**, *127*, 230–239. [[CrossRef](#)]
68. Borisova, D.; Akçakayiran, D.; Schenderlein, M.; Möhwald, H.; Shchukin, D.G. Nanocontainer-based anticorrosive coatings: Effect of the container size on the self-healing performance. *Adv. Funct. Mater.* **2013**, *23*, 3799–3812. [[CrossRef](#)]
69. Shang, X.Y.; Zhu, Z.K.; Yin, J.; Ma, X.D. Compatibility of soluble polyimide/silica hybrids induced by a coupling agent. *Chem. Mater.* **2002**, *14*, 71–77. [[CrossRef](#)]
70. Zhang, S.; Yu, A.; Song, X.; Liu, X. Synthesis and characterization of waterborne UV-curable polyurethane nanocomposites based on the macromonomer surface modification of colloidal silica. *Prog. Org. Coat.* **2013**, *76*, 1032–1039. [[CrossRef](#)]
71. Rusmirović, J.D.; Trifković, K.T.; Bugarski, B.; Pavlović, V.B.; Džunuzović, J.; Tomić, M.; Marinković, A.D. High performance unsaturated polyester based nanocomposites: Effect of vinyl modified nanosilica on mechanical properties. *Express Polym. Lett.* **2016**, *10*, 139–159. [[CrossRef](#)]
72. Qu, A.; Wen, X.; Pi, P.; Cheng, J.; Yang, Z. Synthesis of composite particles through emulsion polymerization based on silica/fluoroacrylate-siloxane using anionic reactive and nonionic surfactants. *J. Colloid Interface Sci.* **2008**, *317*, 62–69. [[CrossRef](#)]
73. Maghami, S.; Dierkes, W.K.; Noordermeer, J.W.M. Functionalized SBRs in silica-reinforced tire tread compounds: Evidence for interactions between filler and zinc oxide. *Rubber Chem. Technol.* **2016**, *89*, 559–572. [[CrossRef](#)]
74. Meador, M.A.B.; Scherzer, C.M.; Vivod, S.L.; Quade, D.; Nguyen, B.N. Epoxy reinforced aerogels made using a streamlined process. *ACS Appl. Mater. Interfaces* **2010**, *2*, 2162–2168. [[CrossRef](#)]
75. Karimi, A.A.; Ahmad, Z. Effect of interface on the thermal mechanical properties of chemically bonded epoxy-silica hybrids. *Prog. Org. Coat.* **2017**, *106*, 137–144. [[CrossRef](#)]
76. Ammar, S.; Ramesh, K.; Ma, I.A.W.; Farah, Z.; Vengadaesvaran, B.; Ramesh, S.; Arof, A.K. Studies on SiO<sub>2</sub>-hybrid polymeric nanocomposite coatings with superior corrosion protection and hydrophobicity. *Surf. Coat. Technol.* **2017**, *324*, 536–545. [[CrossRef](#)]
77. Barna, E.; Bommer, B.; Kürsteiner, J.; Vital, A.; Trzebiatowski, O.V.; Koch, W.; Schmid, B.; Graule, T. Innovative, scratch proof nanocomposites for clear coatings. *Compos. Part A Appl. Sci. Manuf.* **2005**, *36*, 473–480. [[CrossRef](#)]
78. Santiago, A.M.; Ribeiro, T.; Rodrigues, A.S.; Ribeiro, B.; Frade, R.F.M.; Baleizão, C.; Farinha, J.P.S. Multifunctional Hybrid Silica Nanoparticles with a Fluorescent Core and Active Targeting Shell for Fluorescence Imaging Biodiagnostic Applications. *Eur. J. Inorg. Chem.* **2015**, *2015*, 4579–4587. [[CrossRef](#)]
79. Khabibullin, A.; Kopeč, M.; Matyjaszewski, K. Modification of Silica Nanoparticles with Miktoarm Polymer Brushes via ATRP. *J. Inorg. Organomet. Polym. Mater.* **2016**, *26*, 1292–1300. [[CrossRef](#)]
80. Tawiah, B.; Zhang, L.; Tian, A.; Fu, S.S. Coloration of aluminum pigment using SiO<sub>2</sub> and  $\gamma$ -glycidoxypropyltrimethoxysilane with dichlorotriazine reactive dye. *Pigment. Resin Technol.* **2016**, *45*, 335–345. [[CrossRef](#)]
81. Acebo, C.; Fernández-Francos, X.; Santos, J.I.; Messori, M.; Ramis, X.; Serra, À. Hybrid epoxy networks from ethoxysilyl-modified hyperbranched poly(ethyleneimine) and inorganic reactive precursors. *Eur. Polym. J.* **2015**, *70*, 18–27. [[CrossRef](#)]

82. Yang, L.; Jiang, H.; Shen, Y.; Zhou, L. Antireflection coating on silk fabric fabricated from reactive silica nanoparticles and its deepening color performance. *J. Sol. Gel Sci. Technol.* **2015**, *74*, 488–498. [[CrossRef](#)]
83. Wang, H.; Fu, Z.; Zhao, X.; Li, Y.; Li, J. Reactive Nanoparticles Compatibilized Immiscible Polymer Blends: Synthesis of Reactive SiO<sub>2</sub> with Long Poly(methyl methacrylate) Chains and the in Situ Formation of Janus SiO<sub>2</sub> Nanoparticles Anchored Exclusively at the Interface. *ACS Appl. Mater. Interfaces* **2017**, *9*, 14358–14370. [[CrossRef](#)] [[PubMed](#)]
84. Zhi, D.; Wang, H.; Jiang, D.; Parkin, I.P.; Zhang, X. Reactive silica nanoparticles turn epoxy coating from hydrophilic to super-robust superhydrophobic. *RSC Adv.* **2019**, *9*, 12547–12554. [[CrossRef](#)]
85. Türünc, O.; Kayaman-Apohan, N.; Kahraman, M.V.; Menciloğlu, Y.; Güngör, A. Nonisocyanate based polyurethane/silica nanocomposites and their coating performance. *J. Sol. Gel Sci. Technol.* **2008**, *47*, 290–299. [[CrossRef](#)]
86. Radhakrishnan, B.; Constable, A.N.; Brittain, W.J. A novel route to organic-inorganic hybrid nanomaterials. *Macromol. Rapid Commun.* **2008**, *29*, 1828–1833. [[CrossRef](#)]
87. Huang, Y.; Morinaga, T.; Tai, Y.; Tsujii, Y.; Ohno, K. Immobilization of semisoft colloidal crystals formed by polymer-brush-aided hybrid particles. *Langmuir* **2014**, *30*, 7304–7312. [[CrossRef](#)]
88. Ribeiro, T.; Baleizão, C.; Farinha, J.P.S. Synthesis and Characterization of Perylenediimide Labeled Core-Shell Hybrid Silica-Polymer Nanoparticles. *J. Phys. Chem. C* **2009**, *113*, 18082–18090. [[CrossRef](#)]
89. Schoth, A.; Adurahim, E.S.; Bahattab, M.A.; Landfester, K.; Muñoz-Espí, R. Waterborne Polymer/Silica Hybrid Nanoparticles and Their Structure in Coatings. *Macromol. React. Eng.* **2016**, *10*, 47–54. [[CrossRef](#)]
90. Riazi, H.; Jalali-Arani, A.; Afshar Taromi, F. In situ synthesis of silica/polyacrylate nanocomposite particles simultaneously bearing carboxylate and sulfonate functionalities via soap-free seeded emulsion polymerization. *Mater. Chem. Phys.* **2018**, *207*, 470–478. [[CrossRef](#)]
91. Kim, J.W.; Kim, L.U.; Kim, C.K. Size control of silica nanoparticles and their surface treatment for fabrication of dental nanocomposites. *Biomacromolecules* **2007**, *8*, 215–222. [[CrossRef](#)] [[PubMed](#)]
92. Wouters, M.E.L.; Wolfs, D.P.; Van Der Linde, M.C.; Hovens, J.H.P.; Tinnemans, A.H.A. Transparent UV curable antistatic hybrid coatings on polycarbonate prepared by the sol-gel method. *Prog. Org. Coat.* **2004**, *51*, 312–320. [[CrossRef](#)]
93. Ji, H.; Wang, S.; Yang, X. Preparation of polymer/silica/polymer tri-layer hybrid materials and the corresponding hollow polymer microspheres with movable cores. *Polymer (Guildf)* **2009**, *50*, 133–140. [[CrossRef](#)]
94. Lee, C.K.; Don, T.M.; Lai, W.C.; Chen, C.C.; Lin, D.J.; Cheng, L.P. Preparation and properties of nano-silica modified negative acrylate photoresist. *Thin Solid Films* **2008**, *516*, 8399–8407. [[CrossRef](#)]
95. Song, T.; Liu, T.; Yang, X.; Bai, F. Raspberry-like particles via the heterocoagulated reaction between reactive epoxy and amino groups. *Colloids Surf. A Physicochem. Eng. Asp.* **2015**, *469*, 60–65. [[CrossRef](#)]
96. Liang, J.; Wang, L.; Bao, J.; He, L. SiO<sub>2</sub>-g-PS/fluoroalkylsilane composites for superhydrophobic and highly oleophobic coatings. *Colloids Surf. A Physicochem. Eng. Asp.* **2016**, *507*, 26–35. [[CrossRef](#)]
97. Sarsabili, M.; Kalantari, K.; Khezri, K. SR&NI atom transfer radical random copolymerization of styrene and butyl acrylate in the presence of MPS-functionalized silica aerogel nanoparticles: Investigating thermal properties. *J. Therm. Anal. Calorim.* **2016**, *126*, 1261–1272. [[CrossRef](#)]
98. Weng, C.J.; Chen, Y.L.; Jhuo, Y.S.; Yi-Li, L.; Yeh, J.M. Advanced antistatic/anticorrosion coatings prepared from polystyrene composites incorporating dodecylbenzenesulfonic acid-doped SiO<sub>2</sub>@polyaniline core-shell microspheres. *Polym. Int.* **2013**, *62*, 774–782. [[CrossRef](#)]
99. Liu, S.; Han, M. Synthesis, functionalization, and bioconjugation of monodisperse, silica-coated gold nanoparticles: Robust bioprobes. *Adv. Funct. Mater.* **2005**, *15*, 961–967. [[CrossRef](#)]
100. Jouyandeh, M.; Jazani, O.M.; Navarchian, A.H.; Shabaniyan, M.; Vahabi, H.; Saeb, M.R. Surface engineering of nanoparticles with macromolecules for epoxy curing: Development of super-reactive nitrogen-rich nanosilica through surface chemistry manipulation. *Appl. Surf. Sci.* **2018**, *447*, 152–164. [[CrossRef](#)]
101. Xu, J.; Bartels, J.W.; Bohnsack, D.A.; Tseng, T.C.; Mackay, M.E.; Wooley, K.L. Hierarchical inorganic-organic nanocomposites possessing amphiphilic and morphological complexities: Influence of nanofiller dispersion on mechanical performance. *Adv. Funct. Mater.* **2008**, *18*, 2733–2744. [[CrossRef](#)]
102. Kumar, V.; Misra, N.; Paul, J.; Bhardwaj, Y.K.; Goel, N.K.; Francis, S.; Sarma, K.S.S.; Varshney, L. Organic/inorganic nanocomposite coating of bisphenol A diglycidyl ether diacrylate containing silica nanoparticles via electron beam curing process. *Prog. Org. Coat.* **2013**, *76*, 1119–1126. [[CrossRef](#)]
103. Hood, M.A.; Mari, M.; Muñoz-Espí, R. Synthetic strategies in the preparation of polymer/inorganic hybrid nanoparticles. *Materials* **2014**, *7*, 4057–4087. [[CrossRef](#)] [[PubMed](#)]
104. Ma, M.; Zheng, S.; Chen, H.; Yao, M.; Zhang, K.; Jia, X.; Mou, J.; Xu, H.; Wu, R.; Shi, J. A combined “RAFT” and “Graft From” polymerization strategy for surface modification of mesoporous silica nanoparticles: Towards enhanced tumor accumulation and cancer therapy efficacy. *J. Mater. Chem. B* **2014**, *2*, 5828–5836. [[CrossRef](#)] [[PubMed](#)]
105. Gonçalves, J.L.M.; Castanheira, E.J.; Alves, S.P.C.; Baleizão, C.; Farinha, J.P. Grafting with RAFT-gRAFT strategies to prepare hybrid nanocarriers with core-shell architecture. *Polymers* **2020**, *12*, 2175. [[CrossRef](#)] [[PubMed](#)]
106. Asai, M.; Zhao, D.; Kumar, S.K. Role of Grafting Mechanism on the Polymer Coverage and Self-Assembly of Hairy Nanoparticles. *ACS Nano* **2017**, *11*, 7028–7035. [[CrossRef](#)]
107. Matyjaszewski, K.; Spanswick, J. Controlled/living radical polymerization. *Mater. Today* **2005**, *8*, 26–33. [[CrossRef](#)]

108. Czarnecki, S.; Bertin, A. Hybrid Silicon-Based Organic/Inorganic Block Copolymers with Sol–Gel Active Moieties: Synthetic Advances, Self-Assembly and Applications in Biomedicine and Materials Science. *Chem. Eur. J.* **2018**, *24*, 3354–3373. [[CrossRef](#)] [[PubMed](#)]
109. Rodrigues, A.S.; Ribeiro, T.; Fernandes, F.; Farinha, J.P.S.; Baleizão, C. Intrinsically fluorescent silica nanocontainers: A promising theranostic platform. *Microsc. Microanal.* **2013**, *19*, 1216–1221. [[CrossRef](#)] [[PubMed](#)]
110. Tumnantong, D.; Rempel, G.L.; Prasassarakich, P. Polyisoprene-silica nanoparticles synthesized via RAFT emulsifier-free emulsion polymerization using water-soluble initiators. *Polymers* **2017**, *9*, 637. [[CrossRef](#)] [[PubMed](#)]
111. Gonçalves, J.L.M.; Crucho, C.I.C.; Alves, S.P.C.; Baleizão, C.; Farinha, J.P.S. Hybrid mesoporous nanoparticles for pH-actuated controlled release. *Nanomaterials* **2019**, *9*, 483. [[CrossRef](#)]
112. Désert, A.; Chaduc, I.; Fouilloux, S.; Taveau, J.C.; Lambert, O.; Lansalot, M.; Bourgeat-Lami, E.; Thill, A.; Spalla, O.; Ravaine, S.; et al. High-yield preparation of polystyrene/silica clusters of controlled morphology. *Polym. Chem.* **2012**, *3*, 1130–1132. [[CrossRef](#)]
113. Parvole, J.; Chaduc, I.; Ako, K.; Spalla, O.; Thill, A.; Ravaine, S.; Duguet, E.; Lansalot, M.; Bourgeat-Lami, E. Efficient synthesis of snowman- and dumbbell-like silica/polymer anisotropic heterodimers through emulsion polymerization using a surface-anchored cationic initiator. *Macromolecules* **2012**, *45*, 7009–7018. [[CrossRef](#)]
114. Reculusta, S.; Poncet-Legrand, C.; Ravaine, S.; Mingotaud, C.; Duguet, E.; Bourgeat-Lami, E. Syntheses of raspberry-like silica/polystyrene materials. *Chem. Mater.* **2002**, *14*, 2354–2359. [[CrossRef](#)]
115. Mehlhase, S.; Schäfer, C.G.; Morsbach, J.; Schmidt, L.; Klein, R.; Frey, H.; Gallei, M. Vinylphenylglycidyl ether-based colloidal architectures: High-functionality crosslinking reagents, hybrid raspberry-type particles and smart hydrophobic surfaces. *RSC Adv.* **2014**, *4*, 41348–41352. [[CrossRef](#)]
116. Bourgeat-Lami, E.; França, A.J.P.G.; Chaparro, T.C.; Silva, R.D.; Dugas, P.Y.; Alves, G.M.; Santos, A.M. Synthesis of polymer/silica hybrid latexes by surfactant-free RAFT-mediated emulsion polymerization. *Macromolecules* **2016**, *49*, 4431–4440. [[CrossRef](#)]
117. Gan, S.; Yang, P.; Yang, W. Interface-directed sol-gel: Direct fabrication of the covalently attached ultraflat inorganic oxide pattern on functionalized plastics. *Sci. China Chem.* **2010**, *53*, 173–182. [[CrossRef](#)]
118. Abenojar, J.; Tutor, J.; Ballesteros, Y.; del Real, J.C.; Martínez, M.A. Erosion-wear, mechanical and thermal properties of silica filled epoxy nanocomposites. *Compos. Part B Eng.* **2017**, *120*, 42–53. [[CrossRef](#)]
119. Wang, S.C.; Chen, P.C.; Peng, C.J.; Hwang, J.Z.; Chen, K.N. Flame retardation behaviors of UV-curable phosphorus-containing PU coating system. *J. Polym. Eng.* **2013**, *33*, 749–756. [[CrossRef](#)]
120. Sun, D.; Zhang, Y. Preparation of fast-drying waterborne nano-complex traffic-marking paint. *J. Coat. Technol. Res.* **2012**, *9*, 151–156. [[CrossRef](#)]
121. Yang, Y.; Yu, W.; Duan, H.; Liu, Y.; Wang, X.; Yang, J. Realization of reinforcing and toughening poly (phenylene sulfide) with rigid silica nanoparticles. *J. Polym. Res.* **2016**, *23*. [[CrossRef](#)]
122. Sbardella, F.; Bracciale, M.P.; Santarelli, M.L.; Asua, J.M. Progress in Organic Coatings Waterborne modified-silica/acrylates hybrid nanocomposites as surface protective coatings for stone monuments. *Prog. Org. Coat.* **2020**, *149*, 105897. [[CrossRef](#)]
123. Karamanolevski, P.; Buzarovska, A.; Bogoeva-gaceva, G. The Effect of Curing Agents on Basic Properties of Silicone-epoxy Hybrid Resin. *Silicon* **2018**, *10*, 2915–2925. [[CrossRef](#)]
124. Shen, K.; Yu, M.; Li, Q.; Sun, W.; Zhang, X.; Quan, M.; Liu, Z.; Shi, S.; Gong, Y. Synthesis of a fluorine-free polymeric water-repellent agent for creation of superhydrophobic fabrics. *Appl. Surf. Sci.* **2017**, *426*, 694–703. [[CrossRef](#)]
125. Zhang, G.; Kataphinan, W.; Teye-Mensah, R.; Katta, P.; Khatri, L.; Evans, E.A.; Chase, G.G.; Ramsier, R.D.; Reneker, D.H. Electrospun nanofibers for potential space-based applications. *Mater. Sci. Eng. B Solid State Mater. Adv. Technol.* **2005**, *116*, 353–358. [[CrossRef](#)]
126. Dong, H.; Ye, P.; Zhong, M.; Pietrasik, J.; Drumright, R.; Matyjaszewski, K. Superhydrophilic Surfaces via Polymer–SiO<sub>2</sub> Nanocomposites. *Langmuir* **2010**, *26*, 15567–15573. [[CrossRef](#)]
127. Zhao, L.; Yan, X.; Jie, Z.; Yang, H.; Yang, S.; Liang, J. Regenerable antimicrobial N-halamine/silica hybrid nanoparticles. *J. Nanopart. Res.* **2014**, *16*, 2454. [[CrossRef](#)]
128. Akram, D.; Hakami, O.; Sharmin, E.; Ahmad, S. Castor and Linseed oil polyurethane/TEOS hybrids as protective coatings: A synergistic approach utilising plant oil polyols, a sustainable resource. *Prog. Org. Coat.* **2017**, *108*, 1–14. [[CrossRef](#)]
129. Kawahara, T.; Takeuchi, Y.; Wei, G.; Shirai, K.; Yamauchi, T.; Tsubokawa, N. Preparation of Antibacterial Polymer-grafted Silica Nanoparticle and Surface Properties of Composite Filled with the Silica (2). *Polym. J.* **2009**, *41*, 744–751. [[CrossRef](#)]
130. Il'ina, M.A.; Mashlyakovskii, L.N.; Drinberg, A.S.; Khomko, E.V.; Garabadzhiu, A.V. Silicon-Containing Epoxy Composites and Their Use in Marine Coatings Technology. *Russ. J. Appl. Chem.* **2019**, *92*, 530–542. [[CrossRef](#)]
131. Yamashita, R.; Takeuchi, Y.; Kikuchi, H.; Shirai, K.; Yamauchi, T.; Tsubokawa, N. Preparation of Antibacterial Polymer-grafted Nano-sized Silica and Surface Properties of Silicone Rubber Filled with the Silica. *Polym. J.* **2006**, *38*, 844–851. [[CrossRef](#)]
132. Guo, R.; Chen, X.; Zhu, X.; Dong, A.; Zhang, J. A facile strategy to fabricate covalently linked raspberry-like nanocomposites with pH and thermo tunable structures. *RSC Adv.* **2016**, *6*, 40991–41001. [[CrossRef](#)]
133. Hao, L.F.; An, Q.F.; Xu, W.; Wang, Q.J. Synthesis of fluoro-containing superhydrophobic cotton fabric with washing resistant property using nano-SiO<sub>2</sub> sol-gel method. *Adv. Mater. Res.* **2010**, *121–122*, 23–26. [[CrossRef](#)]
134. Nahum, T.; Dodiuk, H.; Dotan, A.; Kenig, S.; Lellouche, J.P. Durable bonding of silica nanoparticles to polymers by photoradiation for control of surface properties. *Polym. Adv. Technol.* **2014**, *25*, 723–731. [[CrossRef](#)]

135. Nahum, T.; Dodiuk, H.; Dotan, A.; Kenig, S.; Lellouche, J.P. Superhydrophobic durable coating based on UV-photoreactive silica nanoparticles. *AIP Conf. Proc.* **2015**, *1664*, 070001. [[CrossRef](#)]
136. Jennings, A.R.; Budy, S.M.; Thrasher, C.J.; Iacono, S.T. Synthesis of fluorinated silica nanoparticles containing latent reactive groups for post-synthetic modification and for tunable surface energy. *Nanoscale* **2016**, *8*, 16212–16220. [[CrossRef](#)] [[PubMed](#)]
137. Xu, L.; Shen, Y.; Wang, L.; Ding, Y.; Cai, Z. Preparation of vinyl silica-based organic/inorganic nanocomposites and superhydrophobic polyester surfaces from it. *Colloid Polym. Sci.* **2015**, *293*, 2359–2371. [[CrossRef](#)]
138. Cho, E.C.; Chang-Jian, C.W.; Chen, H.C.; Chuang, K.S.; Zheng, J.H.; Hsiao, Y.S.; Lee, K.C.; Huang, J.H. Robust multifunctional superhydrophobic coatings with enhanced water/oil separation, self-cleaning, anti-corrosion, and anti-biological adhesion. *Chem. Eng. J.* **2017**, *314*, 347–357. [[CrossRef](#)]
139. Nikolic, M.; Sanadi, A.R.; Lof, D.; Barsberg, S.T. Influence of colloidal nano-silica on alkyd autoxidation. *J. Mater. Sci.* **2017**, *52*, 7158–7165. [[CrossRef](#)]
140. Sharmin, E.; Zafar, F.; Akram, D.; Alam, M.; Ahmad, S. Recent advances in vegetable oils based environment friendly coatings: A review. *Ind. Crops Prod.* **2015**, *76*, 215–229. [[CrossRef](#)]
141. Theodoratou, A.; Bonnet, L.; Dieudonné, P.; Massiera, G.; Etienne, P.; Robin, J.J.; Lapinte, V.; Chopineau, J.; Oberdisse, J.; Aubert-Pouëssel, A. Vegetable oil hybrid films cross-linked at the air-water interface: Formation kinetics and physical characterization. *Soft Matter* **2017**, *13*, 4569–4579. [[CrossRef](#)] [[PubMed](#)]
142. Tian, P.; Guo, Z. Bioinspired silica-based superhydrophobic materials. *Appl. Surf. Sci.* **2017**, *426*, 1–18. [[CrossRef](#)]
143. Giamberini, M.; Malucelli, G. Hybrid organic-inorganic UV-cured films containing liquid-crystalline units. *Thin Solid Films* **2013**, *548*, 150–156. [[CrossRef](#)]